CrystEngComm

Accepted Manuscript

This is an *Accepted Manuscript*, which has been through the Royal Society of Chemistry peer review process and has been accepted for publication.

Accepted Manuscripts are published online shortly after acceptance, before technical editing, formatting and proof reading. Using this free service, authors can make their results available to the community, in citable form, before we publish the edited article. We will replace this *Accepted Manuscript* with the edited and formatted *Advance Article* as soon as it is available.

You can find more information about *Accepted Manuscripts* in the Information for Authors.

ROYAL SOCIETY OF CHEMISTRY

www.rsc.org/crystengcomm

CrystEngComm

ARTICLE

Selective Growth of TiO$_2$ Beads on Ag Nanowires and Their Photocatalytic Performance

Changchao Jia,[a] Hsueh-Shih Chen[b] and Ping Yang*[a]

In this paper, TiO$_2$ beads were deposited on Ag nanowires to create a necklace-like Ag nanowire@TiO$_2$ (Ag NW@TiO$_2$) heterostructure for the first time. It was fabricated via a two-step synthetic method, including the preparation of uniform Ag NWs and the deposition of TiO$_2$ on the Ag surface. Thioglycolic acid (TGA) molecule was used as a bonding agent to solve the thorny issue of substantial lattice mismatch between Ag NW core and TiO$_2$ shell. The amount of water and the permittivity of the solvents are found to be important factors for forming the necklace-like heterostructure. Moreover, by varying the amount of titanium butoxide (TBT), the diameter of the TiO$_2$ beads can be feasibly changed. The photocatalytic performance of the necklace-like Ag NW@TiO$_2$ was evaluated via degradation of methyl orange (MO) under ultraviolet (UV) light. The results reveal that the molar ratio of TiO$_2$ to Ag plays the synergistic effect on the photocatalytic activity, and the best Ti/Ag ratio is found to be 2.8 for the highest photocatalytic performance for Ag NW@TiO$_2$ heterostructure.

Introduction

In recent years, metal and semiconductor composite systems have received intensive attention because of their unique properties and potential applications.[1-4] To date, various metal–semiconductor nanocomposites with complex structures and dimensions have been fabricated such as the delicate combination of Au/TiO$_2$,[5] Ag/TiO$_2$,[6] Pt/TiO$_2$,[7] Au/ZnO,[8] Ag/ZnO,[9] Au/Fe$_2$O$_3$,[10] Ag/Fe$_2$O$_3$,[11] Au/CeO$_2$,[12] Au/Cu$_2$O,[13] and Ag/AgCl.[14] Among the various composite systems, Ag and TiO$_2$ heterostructure is one of the most widely researched materials. Not only Ag nanomaterials possess localized surface plasmon resonance,[15] surface-enhanced Raman scattering (SERS),[16] and metal-enhanced fluorescence,[17] but also TiO$_2$ has the wide applications in solar energy conversion,[18] photoelectrochemical activity,[19] photocatalytic water splitting,[20] and photocatalysis.[21] Thus, Ag@TiO$_2$ heterostructures can combine the merits of Ag and TiO$_2$, which have potential applications in photocatalysis,[22] biotechnologies,[23] optical devices,[24] and SERS fields.[25]

Various Ag/TiO$_2$ heterostructures have been prepared by researchers.[26-28] Generally speaking, according to the particle size and component distribution, these Ag/TiO$_2$ heterostructures can be mainly classified into three types: Ag nanoparticles/TiO$_2$ nanoparticles,[29] Ag nanoparticles/1D TiO$_2$ (nanotubes, nanowires/nanorods, nanobelts),[26,28,30] and Ag NW/TiO$_2$ nanoparticles.[31] Up to now, a lot of works about TiO$_2$ nanoparticles and nanowires decorated with Ag nanoparticles have been researched. The noble metal nanocrystals were anchored on the surfaces of the semiconductors as isolated "islands". Although the metal/TiO$_2$ (termed as M/TiO$_2$ hereafter) exhibits an enhanced photocatalytic activity, the exposed noble metal is easily corroded or dissolved in the surrounding medium. In order to improve the chemical stability of the noble metal, many researchers have been trying to design and synthesize new heterostructures using noble metal as a core. Xu et al. have synthesized M@TiO$_2$ (M = Au, Pd, Pt) core-shell nanocomposites,[32] exhibiting an excellent photocatalysis chemical activity. Wu et al. reported M@TiO$_2$ (M =Au, Ag, Pt) core-shell nanocomposites with truncated wedge-shaped morphology.[33] However, very few reports focused on the one dimensional (1D) Ag NW combined with TiO$_2$. Considered that Ag nanoparticle cannot efficiently transfer the electrons if they are grown as a core, because the transferred electrons may accumulate in the Ag core that causes suppression of the activity. Since 1D Ag NWs exhibit a great electron-transport property. Tailoring and fabricating TiO$_2$ coated on the Ag NW could be effective in improving the photocatalytic. However, a substantial lattice mismatch exists between Ag and TiO$_2$, and the aspect ratio of the Ag NW is very large. Thus, it is difficult to achieve precisely control over coating of TiO$_2$ on the surface of Ag NW, so a well-defined morphology of Ag NW@TiO$_2$ heterostructure is rarely seen.

Aimed at a large lattice mismatch of two materials, Tarr group applied a novel technology to fabricate TiO$_2$ nanostructures by using commercial anodic aluminum oxide (AAO) membrane with core of Au nanorods. TiO$_2$ nanotubes were first grown in alumina templates using sol-gel method, and then gold NWs were subsequently grown in the pores of these tubes by elecrodeposition.[34] However, the method is rather complicated. The prepared NWs are composed of nanorods or nanoparticles, connecting badly between the nanorods and nanoparticles, which affect the electron transfer in the interior of NW. Du et al. adopted a one-step solution

method to synthesis of Ag@TiO$_2$ core-shell NWs.[35] However, the synthetic process needs a high reaction temperature. Bi group reported that one-diamensional Ag@TiO$_2$ anatase core-shell NWs had been prepared by using PVP and H$_2$O.[36] However, the morphology of the heterosturcture cannot well be precisely controlled. Kim et al. used 2-mercaptoethanol reagents to synthesis of Ag@TiO$_2$ core-shell NWs.[31] However, the surface TiO$_2$ coating of the heterostructures is rough. The anatase TiO$_2$ shell was created from the amorphous phase at high temperature around 500 °C.

Choosing a suitable method or linking reagent is important to synthetic Ag NW@TiO$_2$ heterosturctures. Because Ag can be easily linked to a mercapto group and titanium butoxide (TBT) will possess a hydroxyl group after hydrolysis, we choose a common reagent, which has both mercapto group and carboxyl group, as a bridge to combine Ag NW with TiO$_2$ NPs. Uniform Ag NWs with an average diameter of 40 nm were firstly prepared Ag NWs as the core.[37] And then, thioglycollic acid (TGA) was used as binding agent. The surface of the Ag NW exposes with carboxyl group after a modification by TGA molecules. Subsequently, TBT is added as Ti precursor, to synthetic necklace-like Ag NW@TiO$_2$ heterostructures. The thickness of TiO$_2$ coating can be well regulated by altering the addition amount of TBT. To the best of our knowledge, the novel heterostructures of necklace-like Ag NW@TiO$_2$ are reported here for the first time. The heterostructures revealed a high photocatalytic performance for degradation of methyl orange (MO). The molar ratio of TiO$_2$ to Ag as well as the thickness of TiO$_2$ coating play important roles on the photocatalytic activity.

Experimental

Chemicals

AgNO$_3$ (99.9 %) and PVP (K-30, Mw ~ 40000) were purchased from Shanghai Chemical Reagent Company. Ethanol (AR, ≥ 99.7%), glycerol, and ethylene glycol (EG) were taken from Tianjin Chemical Reagent Company. TBT (AR) and TGA (≥ 98%) were purchased from Aladdin Reagent Company. The de-ionized (DI) water (resistivity ≈ 18 MΩ·cm) was obtained from a Milli-Q synthesis system. All chemicals were used directly without further purification.

Synthesis of Ag NWs

Synthesis of Ag NWs was carried out through the glycerol and EG co-mediated method.[37] In a typical synthesis, 0.067 g of PVP (K-30, Mw ≈ 40 000) was dissolved in a mixture solution of 10 mL glycerol and 3 mL EG. Meanwhile, 0.034 g of AgNO$_3$ was dissolved in 5 mL of glycerol. The above solutions were mixed together and then transferred into a 100 mL Teflon-lined autoclave, followed by solvothermal treatment in an oven at 200 °C for 5 h. The obtained samples were then rinsed with deionized (DI) water (resistivity ≈ 18 MΩ·cm), followed by centrifugation at 4000 rpm to remove excess PVP and polyols. The as-prepared Ag NWs were dispersed in water or ethanol for the next process (the predispersed solvent is very critical for the morphology of the followed synthesized heterostructures).

Synthesis of necklace-like Ag NW@TiO$_2$ heterostructures

As-prepared Ag NWs (0.1 mmol), which had been dispersed in 0.1 mL of DI water, was poured into a beaker containing 20 mL of ethanol. And then 20 μL of TGA was added into the mixture

solution. After stirred for 20 min, 0.1 mL TBT was injected into the solution by dropwise. Stirred for another 20 min, the final mixture was transferred into a 50 mL Teflon-lined autoclave, followed by solvothermal treatment in an oven at 150 °C for 10 h. The obtained samples were washed for 3 times with DI water and centrifuged at 4000 rpm. The preparation conditions of Ag NW@TiO$_2$ samples are listed in Table 1.

Table 1. Preparation condition of Ag NW@TiO$_2$ samples. (as-prepared Ag NWs dispersed in 0.1 mL DI water)

sample	Ag NWs (mmol)	TBT (mL)	TGA (mL)	Ethanol (mL)	n-butanol (mL)
S1	0.1	0.5	0.1	20	-
S2	0.1	0.1	0.02	20	-
S3	0.1	0.05	0.02	20	-
S4	0.1	0.15	0.02	20	-
S5	0.1	0.125	0.02	20	-
S6	0.1	0.075	0.02	20	-
S7	0.1	0.1	-	20	-
S8	0.1	0.1	0.02	5	15

(Note: Reaction temperature was 150 °C and reaction time was 10 h)

Control experiments

In order to detect the role of H$_2$O for forming necklace-like morphology, a series of control experiments were conducted. As-prepared Ag NWs (0.1 mmol), which had been dispersed in ethanol, was poured into a beaker containing 20 mL ethanol or the mixture solution of ethanol and DI water. And then, 20 μL TGA was added into the mixture solution. After stirred for 20 min, 0.1 mL TBT was injected into the solution by dropwise. Stirred for another 20 min, the final mixture was transferred into a 50 mL Teflon-lined autoclave, followed by solvothermal treatment in an oven at 150 °C for 10 h. The preparation conditions of Ag NW@TiO$_2$ samples are listed in Table 2.

Table 2. Preparation condition of Ag NW@TiO$_2$ samples. (as-prepared Ag NWs dispersed in ethanol)

sample	Ag NWs (mmol)	TBT (mL)	TGA (mL)	Ethanol (mL)	H$_2$O (mL)	Time
S9	0.1	0.1	0.02	20	-	10 h
S10	0.1	0.1	0.02	20	-	1 h
S11	0.1	0.1	0.02	20	0.1	30 min
S12	0.1	0.1	0.02	20	0.2	1 h
S9	0.1	0.1	0.02	20	-	10 h

(Note: Reaction temperature was 150 °C)

Characterization

The morphology observation of samples was carried out using a field emission scanning electron microscope (SEM, QUANTA 250 FEG, FEI, America). The transmission electron microscopy (TEM) observation was taken using a JEM-2010 electron microscope, and high-resolution transmission electron microscopy (HRTEM) was recorded by Transmission Electron Microscope (FEI Tecani F20 TEM). The crystal structures and phase composition of samples were identified using an X-Ray Diffraction (XRD) meter (Bruker D8-Advance, Germany). The absorption spectra of samples were characterized by using a conventional UV/Vis spectrometer (Hitachi U-4100).

Photocatalytic tests

The photocatalytic activity was evaluated in the degradation of MO under 20 W ultraviolet (UV) light and 500 W xenon lamp. The distance between the lamp and the target solution was 30 cm. The photocatalyst (0.01 g) was dispersed in 20 mL of MO solution (10 mg·L^{-1}). Prior to irradiation, the suspension was

stirred for 30 min in the dark to ensure the establishment of an adsorption–desorption equilibrium in the working solution. During the photocatalytic degradation process, 2 mL of solution was withdrawn at intervals. The concentration of MO was checked by solution absorbance analysis (UV/Vis spectrometer at room temperature with a quartz cell) at wavelength of 463 nm.

Results and discussion

Formation of necklace-like Ag NW@TiO$_2$ heterostructures

The fabrication of the necklace-like Ag NW@TiO$_2$ heterostructure was carried out via a nonepitaxial growth method. Because of the existence of a substantial lattice mismatch between the materials of Ag and TiO$_2$, epitaxial growth method is not suitable for the preparation of their heterostructures. As a consequence, it is an enormous challenge to prepare well-defined morphology of Ag NW@TiO$_2$ heterostructures. Herein, we firstly obtained the Ag NWs with uniform size, and then used TGA as an adhesive agent to modify the surface of the Ag NWs. Because of TGA molecule has two functional groups, i.e., one is mercapto group and the other is carboxyl group. Considering that Ag can be combined with the mercapto group, and hydrolyzed TBT has at least one hydroxyl group, which can bond to a carboxyl group. Thus, TGA is a suitable reagent as a bridge to combine Ag NW with TiO$_2$ NPs. In order to obtain the necklace-like structure, a small amount of water is introduced in the reaction system. The distribution of water in the solution is uniform because of the existence of TGA in the reaction system. When TBT is added into the reaction solution, those TBT molecules meeting with DI water will hydrolyze relatively fast. Thus, the surface of the Ag NWs will immediately generate an undulating TiO$_2$ coating. Whereafter, hydrolyzates of TBT will deposit on the undulating TiO$_2$ coating. After treated with solvothermal method, TiO$_2$ coated on the Ag NW will transform into anatase phase. As a result, necklace-like Ag NW@TiO$_2$ heterostructures are successfully prepared.
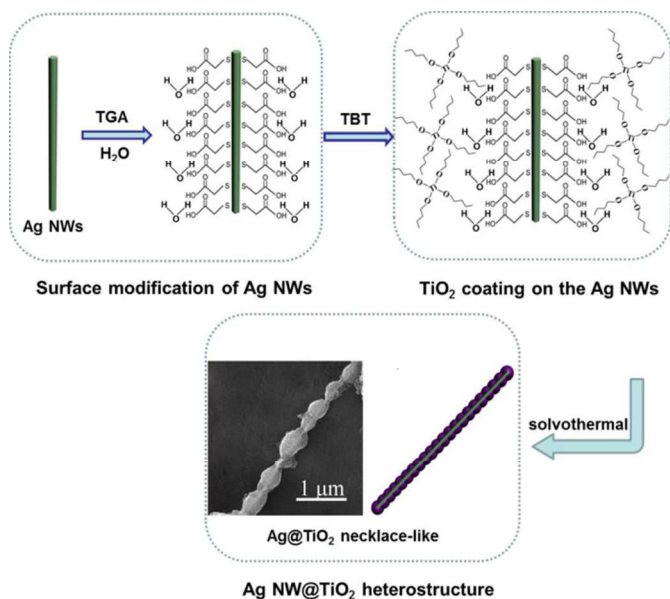
Scheme 1. Schematic for fabrication of necklace-like Ag NW@TiO$_2$ heterostructures.
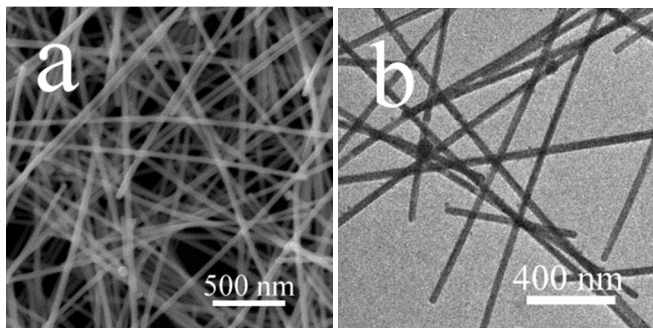
Figure 1. a) SEM and b) TEM images of as-prepared Ag NWs by glycerol and EG co-mediated method.

Ag NWs were firstly prepared by a glycerol and EG co-mediated method reported previously .[37] The morphology of the as-prepared Ag NWs were characterized by using SEM and TEM. Figure 1a shows the SEM image of Ag NWs, revealing that the diameter of synthesized NWs is rather uniform and the length is as long as several micron meters. The mean diameter of the NWs is estimated to be about 40 nm, which can be seen in the TEM image (Figure 1b).
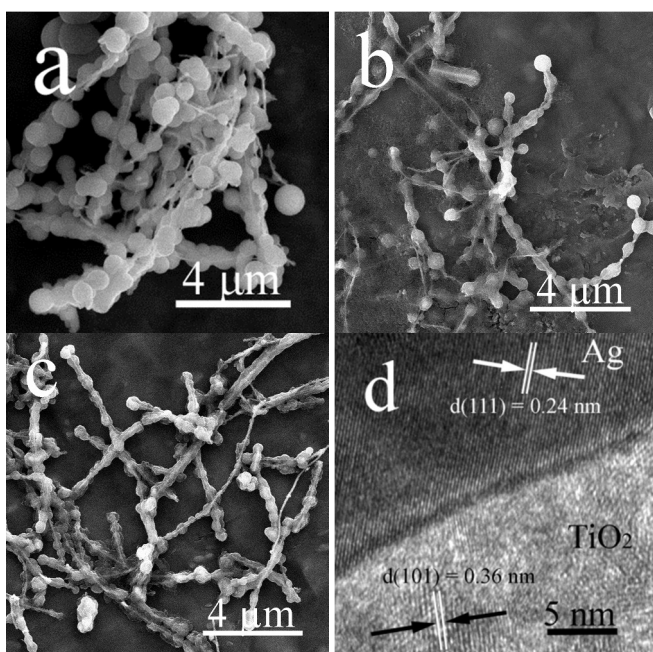
Figure 2. SEM images (a-c) and HRTEM image (d) of Ag NW@TiO$_2$ samples. (a-c) Necklace-like structures prepared with different amounts of TBT: a) 0.5 mL TBT (sample 1), b) 0.1 mL TBT (sample 2), c) 0.05 mL TBT (sample 3), d) HRTEM of sample 2.

The SEM and HRTEM images of the necklace-like Ag NW@TiO$_2$ heterostructures prepared by using TGA as an adhesion agent, which are shown in Figure 2. Large size spheres with an average of 730 nm in diameter are created on the Ag NWs if 0.5 mL TBT is added (Figure 2a). The diameter of the sphere decreases when reducing the amount of TBT. Figure 2b shows the necklace-like Ag NW@TiO$_2$ heterostructures, the diameter of the spheres is about 500 nm. Figure 2c shows that the diameter of the spheres is about 400 nm. It was found that changing the amount of TBT has no obvious influence on the structure of the samples. However, the average size of TiO$_2$ spheres strung on the Ag NWs has changed. In order to further observe the interface boundary of Ag and TiO$_2$, the sample was analysed by HRTEM. Figure 2d

shows the lattice spacing of Ag is 0.24 nm, which corresponds to the (111) planes of Ag, indicating that Ag NWs grow along <110> orientation.[38] The marked interplanar d spacing of TiO_2 is 0.36 nm, which is assigned to the (101) planes of TiO_2, indicating that anatase TiO_2 grown on the Ag NWs have the typical <001> growth direction. The lattice mismatch between Ag and TiO_2 is calculated as ~ 50% according to the ratio of the parameter (shell lattice parameter minus core lattice parameter) to the core lattice parameter.[39]
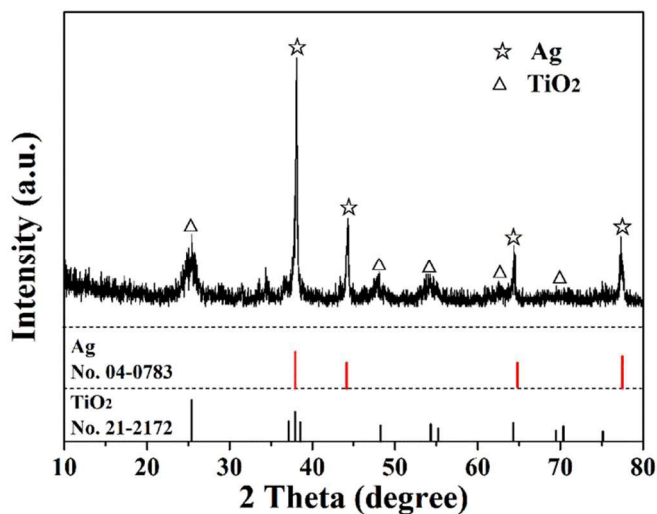
Figure 3. XRD pattern of necklace-like Ag NW@TiO_2 heterostructure (sample 2).

The XRD pattern of necklace-like Ag NW@TiO_2 heterostructure is shown in Figure 3. The result indicates that the diffraction peaks center at 2θ = 38.04°, 44.12°, 64.40°, 77.34°, which agrees with (111), (200), (220), and (311) reflections of the face-centered cubic phase of Ag (JCPDS No. 04-0783), and 2θ = 25.25°, 37.75°, 48.00°, 53.95°, 62.62°, 69.73°, (101), (004), (200), (105), (204), and (220) can be indexed to crystal planes of anatase phase of TiO_2 (JCPDS No. 21-2172).

TGA molecule is considered to be playing an essential role in the formation of Ag NW@TiO_2 heterostructures. Without the modification of Ag NWs surface by TGA molecule, there exists a substantial crystal mismatch between the Ag core and TiO_2 shell. Because a little amount of water exists in the reaction system, the hydrolysis rate of TBT is out of sync. TBT will hydrolyze fast at the site where Ag NWs' surface contacts with relatively much water, leading to the randomly growth of TiO_2 particles on the Ag NW (Figure S2a). The distribution of water in the solution is nonuniform if the reaction system without adding TGA. Furthermore, there is another growth pattern in the reaction system. The phenomenon shown in Figure S2b manifests that TiO_2 small particles deposited on the Ag NWs surface, which can be ascribed to the relatively slow hydrolysis of partial TBT.

As mentioned above, TGA plays an essential role on the morphology of necklace-like heterostructures. Not only TGA can combine with Ag surface by mercapto group, exposing carboxyl group to combine with TBT by specificity bonding, but also it decreases pH valve of the solution,[21] which slows down the hydrolysis rate of TBT to precisely control TiO_2 nanoparticles deposit on the Ag surface. Furthermore, H_2O plays an important role on the formation of necklace-like Ag NW@TiO_2 heterostructures. In order to detect the role of the

water, we stored the as-prepared Ag NWs in the ethanol solution. Ag NW@TiO_2 heterostructures with smooth surface TiO_2 coating are obtained in the absence of water (Figure 4a). In comparison with the morphology (Figure 2), the reason for fabrication of necklace-like Ag NW@TiO_2 heterostructures can be concluded that the hydrolysis rate of TBT is out of sync when a moderate amount of water added into the reaction solution. The surface of the Ag NWs will immediately generate an undulating TiO_2 coating. Subsequently, hydrolyzates of TBT will deposit on the undulating TiO_2 coating. After treated with solvothermal method, necklace-like Ag NW@TiO_2 heterostructures were obtained. From the HRTEM image of the heterostructure (Figure 4b), it indicates that anatase TiO_2 are grown on the Ag NWs along the <001> growth direction. Interestingly, we found that TiO_2 coated on the Ag NW in the same orientation regardless of existence of water in the system. Water only affects the morphology of the Ag NW@TiO_2 heterostructures.
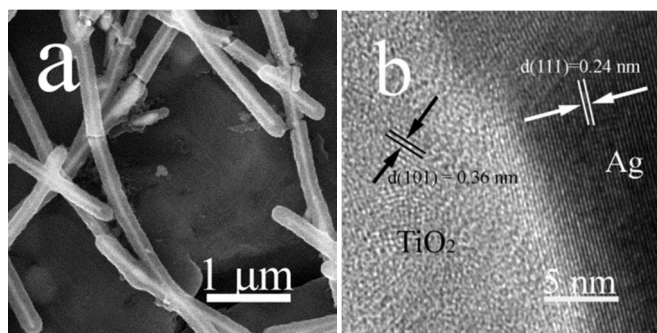
Figure 4. SEM image (a) and HRTEM image (b) of Ag NW@TiO_2 samples prepared in the absence of water (sample 9).
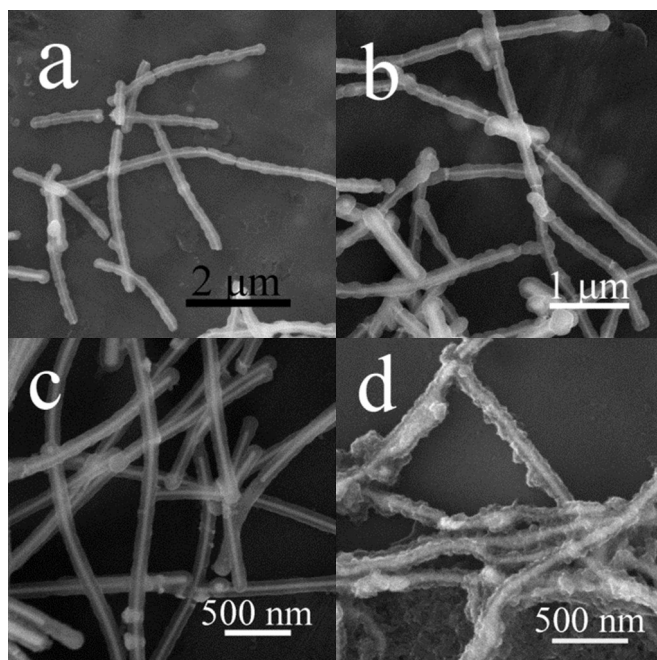
Figure 5. SEM images of Ag NW@TiO_2 heterostructures. a) sample prepared with adding 0.1 mL of DI water for 30 min (sample 11), b) sample prepared with adding 0.2 mL of DI water for 1 h (sample 12), c) sample prepared in the absence of DI water for 1 h (sample 10), d) sample prepared in the mixed solvent of ethanol and n-butanol (sample 8).

When the adding amount of water is 0.1 mL, necklace-like morphology has been formed at the short reaction time (Figure

5a). With increasing the reaction time to 10 h, the size of the TiO$_2$ sphere strung on the Ag NW becomes large, due to the TBT hydrolysis products deposited continuously on the surface of the necklace-like Ag NW@TiO$_2$ (Figure 2b). When increased the amount of water to 0.2 mL, necklace-like Ag NW@TiO$_2$ can also be obtained at reaction time of 1 h (Figure 5b). However, necklace-like morphology is not obvious when increased the amount of water. Polarity of solvents influences the nucleation and growth of the crystals. Because the polarity is positively relate to the dielectric constant, solvents with a higher dielectric constant corresponding to a higher polarity. Thus, the polarity can be seen most easily from the dielectric constants of the solvents. The dielectric constants of water, ethanol, and n-butanol are 80.1, 24.3, and 17.8, respectively. In lower polarity solvents, the interactions would be weaker, leading to less anisotropic growth rates and more equi-axed TiO$_2$ crystals.[40] Consequently, Ag NW@TiO$_2$ heterostructures with smooth surface were obtained in ethanol for 1 h without any water, as shown in Figure 5c. In addition, the necklace-like morphology cannot be obtained in a mixed solution of ethanol and n-butanol, even though Ag NWs has been immersed in the 0.1 mL DI water in advance (as shown in Figure 5d). Thus, necklace-like Ag NW@TiO$_2$ heterostructure can be reproducibly obtained by employing solvents with suitable polarity and by controlling the amount of H$_2$O.
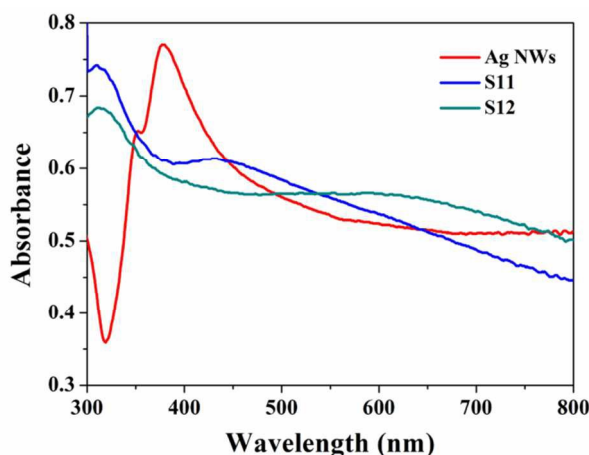
Figure 6. UV-vis absorption spectra of samples.

Optical properties of the necklace-like Ag NW@TiO$_2$ heterostructures and Ag NWs have been studied by taking the UV-vis absorption spectra. The absorption peaks of the materials can be characterized by the UV-vis absorption spectra. The spectra of pure Ag NWs and necklace-like Ag NW@TiO$_2$ heterostructure prepared under reaction time at 30 min (Sample 11), and 1h (sample 12) are shown in Figure 6. Ag NWs display two surface plasmon resonance (SPR) peaks at about 350 and 380 nm. The weaker peak (shoulder peak) at ~ 350 nm corresponds to quadrupole plasmon resonance, while the maximal peak at ~ 380 nm is attributed to transverse resonance excitation.[37] Probably owing to a strong interfacial electronic coupling between neighboring TiO$_2$ nanoparticles and Ag NWs, the surface plasmon band of necklace-like Ag NW@TiO$_2$ heterostructure distinctly broadens and the band shows a red shift compared to that of pure Ag NWs.[41,42] It is noticed that the absorption of necklace-like Ag NW@TiO$_2$ composites is not a simple superposition of individual single-component materials.

Photocatalytic activity of Ag NW@TiO$_2$ heterostrucures

The photocatalytic activity of necklace-like Ag NW@TiO$_2$ heterostructures was evaluated by the degradation of MO under UV irradiation. The degradation profiles of samples with different ratios of Ag and TiO$_2$ are shown in Figure 7. Negative value, the area to the left of the dashed line represents the time used for adsorption–desorption equilibrium. It can be found that the photocatalytic activity of the samples was enhanced with increasing the molar ratio of TiO$_2$ and Ag. At a high molar ratio of TiO$_2$ and Ag (more than 2.8), the photocatalytic activity of the samples decrease again. In order to observe the photocatalytic activity more intuitively and conveniently, the photodegradation rate constant is adopted to describe it. The photocatalytic degradation of MO can be regarded as a pseudo-first order reaction, and its kinetics can be expressed as follows equation: $\ln(C_0/C)=kt$, where C_0 and C are the initial and the reaction concentration of the MO solution, respectively. The apparent photocatalytic degradation rate constant for a sample with S2 is 4.0×10^{-3} min^{-1}, which is higher than that of S3 by a factor of 7.14, than that of S4 by a factor of 2.67. The properties of necklace-like Ag NW@TiO$_2$ heterostructures with different molar ratios of Ti and Ag are listed in Table 3. Compared with the photocatalytic performance of these samples, it can be concluded that the molar ratio of Ag and TiO$_2$ as well as the thickness of TiO$_2$ coating play a synergistic effect on the photocatalytic performance.
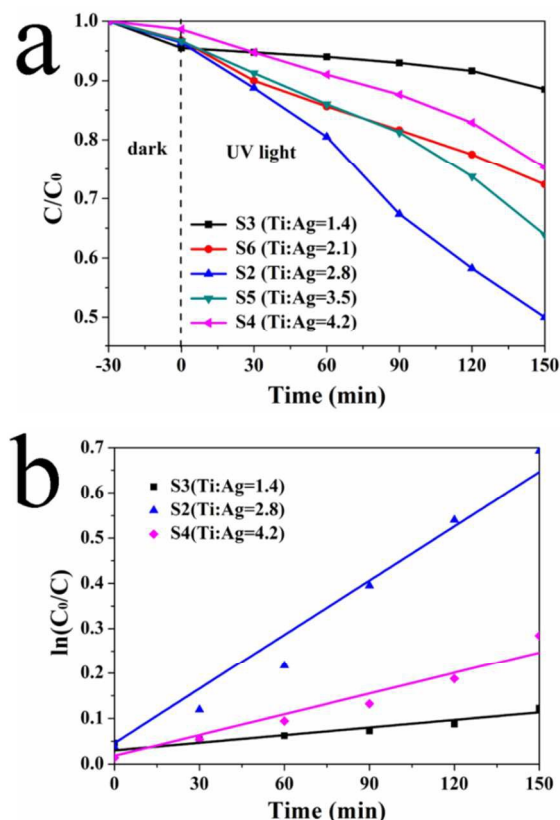
Figure 7. a) Photocatalytic degradation profile of MO under UV irradiation. b) pseudo-first-order kinetic rate plots under UV irradiation.

In addition, the visible-light photocatalytic activity of the sample (S2) for the photodegradation of MO was also examined. The temporal spectral changes and the degradation profile of MO solution during the test process were illustrated

in Figure S3. It is found that the wavelength of the MO solution corresponding to the maximal absorbance (λ_{max}) shifts gradually from the initial 463 nm towards shorter wavelength at 390 nm, along with a gradual decrease in the maximal absorbance during photocatalytic reactions. Although the reason for the movement of the wavelength is not clearly, this is possibly ascribed that the stepwise removal and degradation of MO from the solution.[43,44]

Table 3. Properties of necklace-like Ag NW@TiO₂ heterostructures.

sample	TBT (mL)	Ti/Ag (molar ratio)	Diameter of TiO₂ bead (nm)	TiO₂ coating thickness (nm)	Rate constant K (min⁻¹)
S2	0.1	2.8	500	230	4.0×10^{-3}
S3	0.05	1.4	400	180	5.6×10^{-4}
S4	0.15	4.2	560	260	1.5×10^{-3}

(Note: The diameter of Ag NWs is 40 nm)

Photocatalytic mechanism of Ag NW@TiO₂ heterostrucures
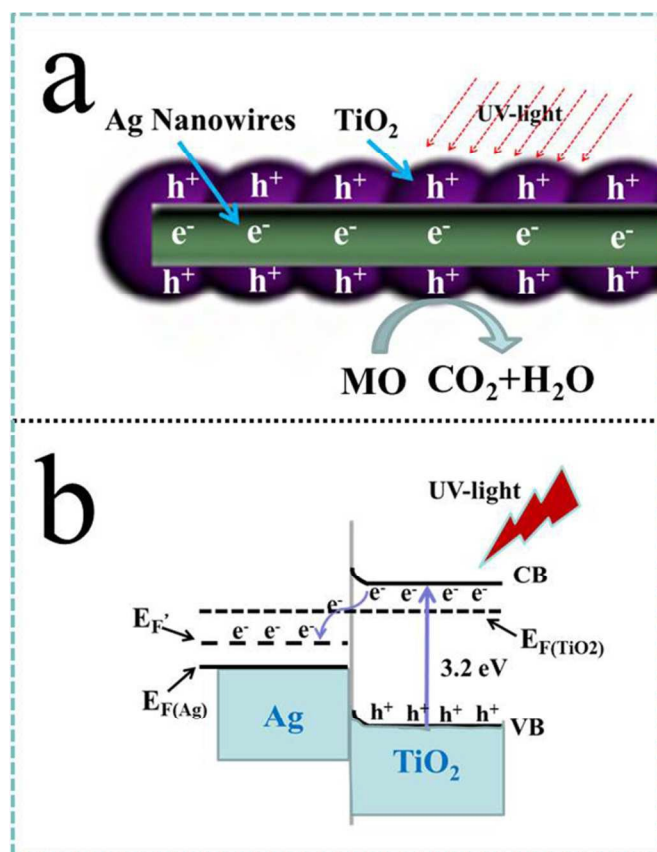
Figure 8. Photocatalytic mechanism of necklace-like Ag NW@TiO₂ heterostructures. a) Charge distribution between Ag NWs core and TiO₂ shell, b) Photo-induced charge separation of necklace-like Ag NW@TiO₂ heterostructures. $E_{F(TiO2)}$ and $E_{F'}$ refer to Fermi levels of TiO₂ before and after attaining equilibrium, $E_{F(Ag)}$ presents the Fermi levels of Ag.

On the basis of the above results, we proposed a possible model to explain that the necklace-like Ag NW@TiO₂ heterostructure exhibits an excellent photocatalytic activity. As shown in Figure 8a, when UV-light illuminates the necklace-like Ag NW@TiO₂ heterostructures, the generated electron-hole pairs are separated into electrons and holes, which could transfer into Ag core and the TiO₂ shell, respectively. Therefore, the recombination of electron and hole would be effectively decreased. Figure 8b gives a possible energy band diagram to

explain the process. When the photon energy of the UV-light higher than or equal to the band gap of TiO₂ crystals, electron (e^-) in the valance band (VB) will be excited to the CB with simultaneous generation of the same amount of holes (h^+) in the VB. And then photoexcited electrons driven by the potential energy, will transfer from TiO₂ shell to Ag core, owing to the Fermi energy of TiO₂ ($E_{F(TiO2)}$) is higher than that of Ag ($E_{F(Ag)}$). Ag NWs not only acts as an electron trap decreasing the recombination rate of photoinduced electron and hole, but also is in favour of the carrier transport in the inner of the Ag NW. Furthermore, an energy barrier, termed as Schottky junction, will be built at the interface of the Ag core and TiO₂ shell. In addition, it prohibits photoinduced carrier recombination, improving the photocatalytic activity of the heterostructures.[7,30]

Conclusions

Necklace-like Ag NW@TiO₂ heterostructures can be easily prepared by a two-step solvothermal method. As-prepared Ag NWs can be firstly synthesized via glycerol and EG co-mediated method. TGA as bonding agents solves the thorny issue of substantial lattice mismatch, resulting in TiO₂ nanoparticles orderly connection on the Ag NW. Regular necklace-like Ag@TiO₂ heterostructure can be well controlled by TGA reagent, and the size of the TiO₂ beads can be easily tuned by adjusting the amount of TBT. The polarity of the solvent plays an important on the morphology of the Ag NW@TiO₂ samples. Furthermore, photocatalytic activity of the samples was measured by degradation of MO. The experimental result reveals that the molar ratio of Ag and TiO₂ as well as the thickness of the shell play a synergistic effect on the photocatalytic performance. This method will be further extended to fabricate other heterostructures with well-defined morphologies for solving the problem of substantial lattice mismatch between two different kinds of materials.

Acknowledgements

Notes and references

ᵃSchool of Material Science and Engineering, University of Jinan, Jinan, 250022, P.R. China.

Fax: +86 531 87974453; Tel: +86 531 89736225

E-mail: mse_yangp@ujn.edu.cn

ᵇDepartment of Materials Science and Engineering, National Tsing Hua University, Hsinchu 300, Taiwan.

† Electronic Supplementary Information (ESI) available: SEM images of Ag NW@TiO₂ samples with different preparation conditions. See DOI: 10.1039/b000000x/

1   S. E. Habas, P. D. Yang and T. J. Mokari, *J. Am. Chem. Soc.*, 2008, **130**, 3294–3295.

2   L. Wu, B. G. Quan, Y. L. Liu, R. Song and Z. Y. Tang, *ACS Nano*, 2011, **5**, 2224–2230.

3   J. Yang and J. Y. Ying, *Angew. Chem. Int. Ed.*, 2011, **50**, 4637–4643.

4   F. R. Fan, Y. Ding, D. Y. Liu, Z. Q. Tian and Z. L. Wang, *J. Am. Chem. Soc.*, 2009, **131**, 12036–12037.

5   W. B. Liang, T. L. Church and A. T. Harris, *Green Chem.*, 2012, **14**, 968–975.

6   N. Perkas, A. Lipovsky, G. Amirian, Y. Nitzan and A. Gedanken, *J. Mater. Chem. B*, 2013, **1**, 5309–5316.

7   H. –S. Chen, P. –H. Chen, S. –H. Huang and T. –P. Perng, *Chem. Commun.*, 2014, **50**, 4379–4382.

8   P. Li, Z. Wei, T. Wu, Q. Peng and Y. D. Li, *J. Am. Chem. Soc.*, 2011, **133**, 5660–5663.

9   D. D. Lin, H. Wu, R. Zhang and W. Pan, *Chem. Mater.*, 2009, **21**, 3479–3484.

10 J. Zhang, X. H. Liu, X. Z. Guo, S. H. Wu and S. R. Wang, *Chem. Eur. J.*, 2010, **16**: 8108-8116.

11 J. S. Jang, K. Y. Yoon, X. Y. Xiao, F. F. Fan and A. J. Bard, *Chem. Mater.*, 2009, **21**, 4803–4810.

12 R. Si and M. Flytzani-Stephanopoulos, *Angew. Chem.*, 2008, **120**, 2926–2929.

13 C. –H. Kuo, T. Hua and M. H. Huang, *J. Am. Chem. Soc.*, 2009, **131**, 17871–17878.

14 C. C. Jia, P. Yang, and B. B. Huang, *ChemCatChem*, 2014, **6**, 611–617.

15 A. J. Haes and R. P. V. Duyne, *J. Am. Chem. Soc.*, 2002, **124**, 10596–10604.

16 A. Tao, F. Kim, C. Hess, J. Goldberger, R. R. He, Y. G. Sun, Y. N. Xia and P. D. Yang, *Nano Lett.*, 2003, **3**, 1229–1233.

17 J. P. Yang, F. Zhang, Y. R. Chen, S. Qian, P. Hu, W. Li, Y. H. Deng, Y. Fang, L. Han, M. Luqman and D. Y. Zhao, *Chem. Commun.*, 2011, **47**, 11618–11620.

18 U. Bach, D. Lupo, P. Comte, J. E. Moser, F. Weissörtel, J. Salbeck, H. Spreitzer and M. Grätzel, *Nature*, 1998, **395**, 583–585.

19 Y. Hou, X. –Y. Li, Q. –D. Zhao, X. Quan and G. –H. Chen, *Adv. Funct. Mater.*, 2010, **20**, 2165–2174.

20 J. W. Tang, J. R. Durrant and D. R. Klug, *J. Am. Chem. Soc.*, 2008, **130**, 13885–13891.

21 C. C. Jia, P. Yang, H.-S. Chen and J. P. Wang, *CrystEngComm*, 2015, **17**, 2940–2948.

22 T. Hirakawa and P. V. Kamat, *J. Am. Chem. Soc.*, 2005, **127**, 3928–3934.

23 S. M. Hussain, L. K. Braydich-Stolle, A. M. Schrand, R. C. Murdock, K. O. Yu, D. M. Mattie, J. J. Schlager and M. Terrones, *Adv. Mater.*, 2009, **21**, 1549–1559.

24 R. T. Tom, A. S. Nair, N. Singh, M. Aslam, C. L. Nagendra, R. Philip, K. Vijayamohanan and T. Pradeep, *Langmuir*, 2003, **19**, 3439–3445.

25 L. B. Yang, X. Jiang, W. D. Ruan, J. X. Yang, B. Zhao, W. Q. Xu and J. R. Lombardi, *J. Phys. Chem. C*, 2009, **113**, 16226–16231.

26 Y. C. Yang, J. W. Wen, J. H. Wei, R. Xiong, J. Shi and C. X. Pan, *ACS Appl. Mater. Inter.*, 2013, **5**, 6201–6207.

27 J. Z. Zhang, X. Liu, S. M. Gao, B. B. Huang, Y. Dai, Y. B. Xu, L. R. Grabstanowicz and T. Xu, *Ceram. Int.* 2013, **39**, 1011–1019.

28 J. X. Li, L. X. Yang, S. L. Luo, B. B. Chen, J. Li, H. L. Lin, Q. Y. Cai and S. Z. Yao, *Anal. Chem.*, 2010, **82**, 7357–7361.

29 S. C. Chan, and M. A. Barteau, *Langmuir*, 2005, **21**, 5588–5595.

30 J. Tian, Z. H. Zhao, A. Kumar, R. I. Boughton and H. Liu, *Chem. Soc. Rev.*, 2014, **43**, 6920–6937.

31 P. Ramasamy, D. –M. Seo, S. –H. Kim and J. Kim, *J. Mater. Chem.*, 2012, **22**, 11651–11657.

32 N. Zhang, S. Q. Liu, X. Z. Fu and Y. –J. Xu, *J. Phys. Chem. C*, 2011, **115**, 9136–9145.

33 X. –F. Wu, H. –Y. Song, J. –M. Yoon, Y. –T. Yu and Y. –F. Chen, *Langmuir*, 2009, **25**, 6438–6447.

34 G. Sahu, S. W. Gordon and M. A. Tarr, *RSC Adv.*, 2012, **2**, 573–582.

35 J. M. Du, J. L. Zhang, Z. M. Liu, B. X. Han, T. Jiang and Y. Huang, *Langmuir*, 2006, **22**, 1307–1312.

36 Q. S. Dong, H. C. Yu, Z. B. Jiao, G. X. Lu and Y. P. Bi, *RSC Adv.*, 2014, **4**, 59114–59117.

37 C. C. Jia, P. Yang and A. Y. Zhang, *Mater. Chem. Phys.*, 2014, **143**, 794–800.

38 J. L. Elechiguerra, L. Larios-Lopez, C. Liu, D. Garcia-Gutierrez, A. Camacho-Bragado and M. J. Yacaman, *Chem. Mater.*, 2005, **17**, 6042–6052.

39 J. T. Zhang, Y. Tang, K. Lee and M. Ouyang, *Science*, 2010, **327**, 1634–1638.

40 L. P. Xu, Y. –L. Hu, C. Pelligra, C.-H. Chen, L. Jin, H. Huang, S. Sithambaram, M. Aindow, R. Joesten and S. L. Suib, *Chem. Mater.*, 2009, **21**, 2875–2885.

41 Z. K. Zheng, B. B. Huang, X. Y. Qin, X. Y. Zhang, Y. Dai and M. –H. Whangbo, *J. Mater. Chem.*, 2011, **21**, 9079–9087.

42 P. Wang, B. B. Huang, Y. Dai and M. –H. Whangbo, *Phys. Chem. Chem. Phys.*, 2012, **14**, 9813–9825.

43 S. W. Liu, K. Yin, W. S. Ren, B. Cheng and J. G. Yu, *J. Mater. Chem.*, 2012, **22**, 17759–17767.

44 D. Zhang, J. Li, Q. G. Wang and Q. S. Wu, *J. Mater. Chem. A*, 2013, **1**, 8622–8629.

CrystEngComm Accepted Manuscript

Selective Growth of TiO₂ Beads on Ag Nanowires and Their Photocatalytic Performance

Changchao Jia,[a] Hsueh-Shih Chen[b] and Ping Yang*[a]

[a]School of Material Science and Engineering, University of Jinan, Jinan, 250022, P.R. China.

Fax: +86 531 87974453; Tel: +86 531 89736225

E-mail: mse_yangp@ujn.edu.cn

[b]Department of Materials Science and Engineering, National Tsing Hua University, Hsinchu 300,

Taiwan.
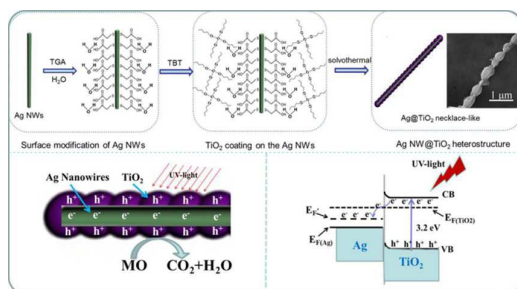
Necklace-like of Ag nanowire@TiO₂ heterostructures were fabricated by a two-step solvothermal method, and exhibited an excellent photocatalytic performance.